Liquid Crystals
Publication details, including instructions for authors and subscription information:
http://www.informaworld.com/smpp/title~content=t713926090

Dynamics of biphotonic intensity holographic gratings based on dye-doped liquid crystal films

Ko-Ting Cheng[a]; Chia-Rong Lee[b]; Andy Ying-Guey Fuh[ab]
[a] Department of Physics, National Cheng Kung University, Taiwan 701, ROC [b] Institute of Electro-Optical Science and Engineering, National Cheng Kung University, Taiwan 701, ROC

To cite this Article Cheng, Ko-Ting , Lee, Chia-Rong and Fuh, Andy Ying-Guey(2007) 'Dynamics of biphotonic intensity holographic gratings based on dye-doped liquid crystal films', Liquid Crystals, 34: 1, 95 — 100
To link to this Article: DOI: 10.1080/02678290601020047
URL: http://dx.doi.org/10.1080/02678290601020047

Liquid Crystals, Vol. 34, No. 1, January 2007, 95–100

Dynamics of biphotonic intensity holographic gratings based on dye-doped liquid crystal films

KO-TING CHENG†, CHIA-RONG LEE‡ and ANDY YING-GUEY FUH*†‡

†Department of Physics, National Cheng Kung University, Tainan, Taiwan 701, ROC
‡Institute of Electro-Optical Science and Engineering, National Cheng Kung University, Tainan, Taiwan 701, ROC

(*Received 24 February 2006; in final form 9 August 2006; accepted 15 August 2006*)

The dynamics of biphotonic intensity holographic gratings (BIHGs) based on dye-doped liquid crystal (DDLC) films, including optical and thermal effects, are studied. Experimental results indicate that the formation of a BIHG involves bulk reorientation and surface adsorption. The former yields a transient biphotonic grating; the latter results in a persistent biphotonic grating. Additionally, the dynamic behaviours of the biphotonic diffraction signals are different from those of a conventional one-photonic diffraction signal, and depend on the intensity(polarization) of the green(red) pump-beam. The effect of ambient temperature on the diffraction efficiency of a BIHG is also studied: a higher ambient temperature prevents more dye molecules from being adsorbed on the substrate.

1. Introduction

Holographic gratings (HGs) formed using two coherent beams from a laser, the so-called one-photonic HGs, have attracted substantial attention over the past decade because of their potential application in optical storage [1–3]. Various materials have been employed to record HGs by exploiting photoinduced anisotropic adsorption effects [2, 3]. Of these, dye-doped liquid crystal (DDLC) films are the most commonly used because of their various photoalignment characteristics [4–8]. In the last few years, HGs, including intensity gratings (IGs) and polarization gratings (PGs) formed using two laser beams of different wavelengths, and termed biphotonic gratings (BGs), have also been studied extensively [9–12]. Various optical materials have been studied in this field. The dynamics of BGs based on azo dye-doped polymers [9–10] and azobenzene [11] were studied by monitoring the self-diffraction signal. This paper presents a dynamic study of biphotonic intensity holographic gratings (BIHGs) in the DDLC system previously reported [12]. To our knowledge, it is the first study to report the dynamics of BIHGs in a DDLC system.

It should be noted that the formation of BIHGs is attributed to dye dichroism, a series of photoisomerization processes, anisotropic adsorption and the inhibition of dye adsorption [4, 7, 13, 14]. BIHGs are generated under the illumination of one linearly polarized green beam with the simultaneous irradiation of an intensity-modulated interference pattern produced by two linearly polarized coherent red beams in DDLC films. The illuminated area in the sample is seen to have periodic green light- and red light-dominant regions. The former(latter) are the low(high) intensity regions of the red interference pattern, and cause a *cis*(*trans*)-rich modulation pattern. The *trans*-isomer with a rod-like shape promotes stabilization of the homogeneous alignment, whereas the bent *cis*-isomer tends to disorganize the LC alignment, lowering the clearing point ($T_{\text{Ch-I}}$) [15]. Therefore, a periodic *trans*-rich/*cis*-rich modulation in the bulk results in a transient phase grating [7, 14], which is called the bulk reorientation effect. In addition, the excited *cis*-MR dyes in the green light-dominant regions then diffuse and are finally adsorbed on the inner command surface of the DDLC cell, with their molecular long axes perpendicular to the polarization direction of the green beam; meanwhile the MR dyes in the red light-dominant regions are adsorbed onto the substrate due to red light-induced *cis–trans* inverse isomerization. The anisotropic adsorbed dyes then reorient the LCs, and form a dye adsorption-induced persistent grating [4, 7]. Thus, the BIHG formed in a DDLC cell exhibits two effects — a bulk reorientation-induced transient grating and a dye adsorption-induced persistent grating.

This work describes the dynamics of BIHGs based on DDLC films, including optical and thermal effects. Additionally, the intensity and direction of polarization

*Corresponding author. Email: andyfuh@mail.ncku.edu.tw

Liquid Crystals
ISSN 0267-8292 print/ISSN 1366-5855 online © 2007 Taylor & Francis
http://www.tandf.co.uk/journals
DOI: 10.1080/02678290601020047

of the green pump-beam relative to that of the red beam are varied to study dynamic behaviour during the formation of a BIHG. The effect of ambient temperature (20–40°C) on this system is also examined. The results obtained indicate that the dynamic behaviour associated with formation of a BIHG significantly depends on the pump-beam intensity, polarization and ambient temperature.

2. Experimental

The nematic liquid crystal and azo dye used in this experiment were E7 (Merck) and methyl red (MR, Aldrich), respectively. MR is a well known azo dye with dichroic ratio, D, defined as $A_{//}/A_{\perp}$ (which approximately is six for visible light), where $A_{//}$ and $A_{\perp}$ are the dye absorbance with the pump polarization parallel and perpendicular, respectively, to the LC optical axis in a homogeneously aligned MR-doped E7 cell. The MR doping concentration was 1 wt%. Each empty cell was fabricated using two indium tin oxide (ITO)-coated glass slides separated by two 12 μm thick plastic spacers. One of the two ITO glass slides was coated with an alignment film, polyvinyl alcohol (PVA), and rubbed in a direction R; the other was not. The surface with (without) a rubbed PVA film is termed the reference (command) surface, S_R (S_C). The homogeneous mixture in the nematic state was injected into an empty cell at room temperature and at normal atmospheric pressure to yield a DDLC film. The LC molecules were aligned with each other near the rubbed reference surface (S_R) and extended through the bulk of the sample to the command surface (S_C) without an alignment film. Homogeneous alignment of the DDLC cell was confirmed using a conoscope.

3. Results and discussion

Figure 1 illustrates the set-up used to record and elucidate the dynamics of a BIHG. Two linearly polarized red beams, E_{R1} and E_{R2}, from a high power He-Ne laser (λ=632.8 nm) were incident onto the sample from S_R with an intersection angle $\theta\sim1°$. These two red pump-beams had the same intensity, $I_{R1,2}\sim180\,mW\,cm^{-2}$, and yielded an intensity-modulated interference field on the DDLC film. Additionally, one linearly polarized (in the y-direction) green beam (Ar^+ laser, λ=514.5 nm), E_G parallel to the direction of rubbing of the substrate R, with an intensity of 6–15 $mW\,cm^{-2}$, was normally incident on the sample from the command surface side. None of the pump beams was focused, and the temperature of the sample was controlled. The evolution of the first order diffraction efficiency was probed using a linearly polarized (E_P, with E_P parallel to the rubbing direction R) low intensity He-Ne laser.

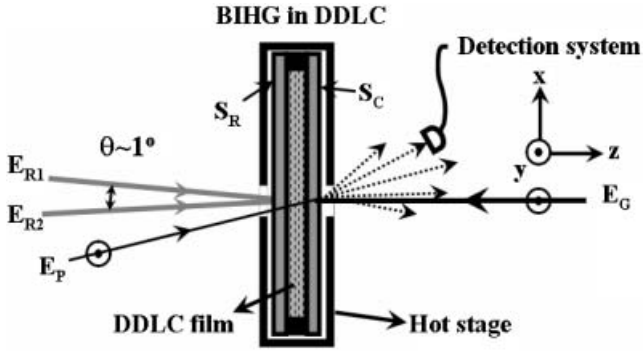

Figure 1. Experimental set-up for the study of the dynamics of BIHGs in DDLC films: S_C=command surface, S_R=reference surface. The polarizations of the red pump beams, E_{R1} and E_{R2}, are parallel. The polarization of the green pump beam, E_G, is in the y-direction. A weak linearly polarized He-Ne beam, E_P (in the y-direction), is used to probe the BIHG formed. The hot stage is used to control the ambient temperature of the DDLC films.

Figure 2 depicts the dynamics of first order diffraction during the formation of a BIHG with $E_R//E_G$ and $E_R\perp E_G$. The intensities of the green and red pump-beams were 7 and 180 $mW\,cm^{-2}$, respectively; the ambient temperature was maintained at a constant ~20°C. The green and red pump-beams were switched on at time t=0 s, and off at t=800 s. Figure 2 clearly shows that first order diffraction efficiency increases with time. When both pump beams are blocked at t=800 s, it then decreases and finally reaches a steady state. The BIHG formation involves two effects — bulk reorientation and surface adsorption. A BIHG is associated (a) with a transient grating, which is a phase grating formed by a periodical *trans*-rich/*cis*-rich modulation in the bulk, and (b) with a persistent grating, which is a twisted nematic (TN) grating formed by LC alignment by the periodically adsorbed dyes on the S_C. As described above, the former, a periodic *trans*-rich/*cis*-rich modulation in the bulk, results in a phase grating, as a result of the bulk-reorientation effect; the latter, with periodically adsorbed dyes on the S_C, generates a surface adsorption grating. When the green and the red pump-beams are switched off, the *cis*-MRs relax back to the stable *trans*-MRs, and the bulk reorientation effect disappears. In other words, the dynamics is due to both the transient grating and the persistent grating before blocking the pump-beams, and it is only generated by the persistent grating after blocking the pump-beams. Accordingly, only the surface adsorption grating contributes to the remaining persistent BIHG component.

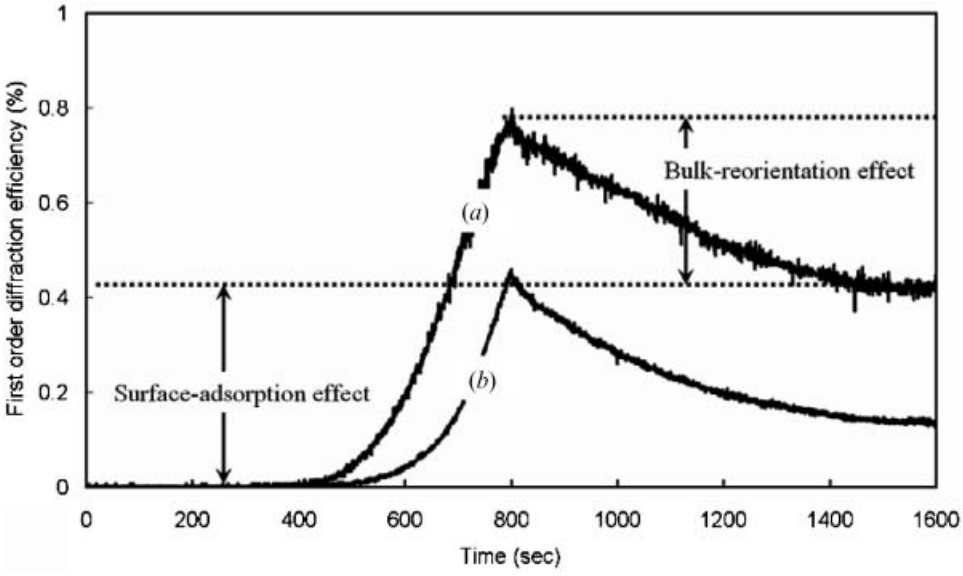

Figure 2. Variation of the dynamics of first order diffraction during the formation of a BIHG with a relative polarization of the red beams, E_R, to that of the green beam, E_G, given by (*a*) $E_R//E_G$ and (*b*) $E_R \perp E_G$. The intensities of the green and the red pump beams are 7 and 180 mW cm^{-2}, respectively. The polarization of the probe beam is parallel to that of the green pump-beam. All pump-beams, except for the probe beam, are turned on(off) at $t=0$ s(800 s).

Furthermore, figure 2 indicates that the diffraction efficiency with $E_R//E_G$ exceeds that with $E_R \perp E_G$ for the persistent BIHG component. The reason is because MRs have a positive dichroic ratio (~6 for visible light), and the long axes of the initial MRs are parallel to E_G. Thus, the *trans*-MRs, which are photoisomerized to *cis*-MRs by green light, absorb more red light with $E_R//E_G$ than with $E_R \perp E_G$. As described in § 1, a higher absorbance of red light would result in much less adsorption of dye due to red light-induced *cis–trans* inverse isomerization. Thus, the green light-induced adsorption effect described above causes the modulation of regions in which dye is or is not adsorbed to be greater in $E_R//E_G$ than in $E_R \perp E_G$.

Illustrations of the anisotropic patterns for the BIHGs under the condition $E_R//E_G$ [$E_R \perp E_G$], with the dynamics presented in figure 2, are shown in figures 3 (*a*, *b*) [3 (*c*, *d*)]. It should be noted that figures 3 (*a*, *c*) [3 (*b*, *d*)] are the patterns obtained when the bulk reorientation effect is present[absent]. The illustration is made based on the theoretical prediction that LCs are reoriented from the homogeneous to TN alignment by the adsorbed MRs in the present case [16, 17]. The twist angle is proportional to the amount of adsorbed dye. As described in § 1, the illuminated area in a BIHG sample can be viewed to have periodic green light- and red light-dominant regions. The former(latter) are the low(high) intensity regions of the red interference pattern, and cause the *cis*(*trans*)-rich modulation pattern. The green light-dominant regions are labelled as E_G-regions; while the red-light dominant regions are designated as E_R+E_G regions, since they are also under the illumination of a green light. Their relative polarizations are set either $E_R//E_G$ or $E_R \perp E_G$. Accordingly, the structures of the inner command surface would have R_1, R_2 and R_3 regions (see figure 3). These regions represent E_G regions (which have strong adsorption of dyes), E_R+E_G regions with $E_R//E_G$ (which have no significant dye adsorption) and E_R+E_G regions with $E_R \perp E_G$ (which have a dye adsorption level between the R_1 and R_2 regions), respectively. The illustration clearly indicates that the index modulation, and thus the combined biphotonic grating effect in figure 3 (*a*) ($E_R//E_G$) would be higher than that in figure 3 (*c*) ($E_R \perp E_G$) when the bulk effect is present. Similarly, figures 3 (*b*) and 3 (*d*) indicate that the remaining BIHG in figure 3 (*b*) (which is a TN grating with $E_R//E_G$) should be higher than that in figure 3 (*d*) (which is a TN grating with $E_R \perp E_G$) after the bulk effect is gone.

The diffraction pattern of the remaining BIHG under conditions the same as for figure 2 (*a*) ($E_R//E_G$), probed using a He-Ne laser, is shown in figure 4 (*a*). Figures 4 (*b*, *c*) are images of the BIHG patterns observed using polarizing optical microscopy (POM) under crossed and parallel polarizers, respectively, and indicate that the grating spacing is ~32 μm. It is clear that the bright(dark) regions in figures 4 (*b*, *c*) are complementary. The bright(dark) regions in figure 4 (*b*) are those with(without) anisotropically adsorbed dye

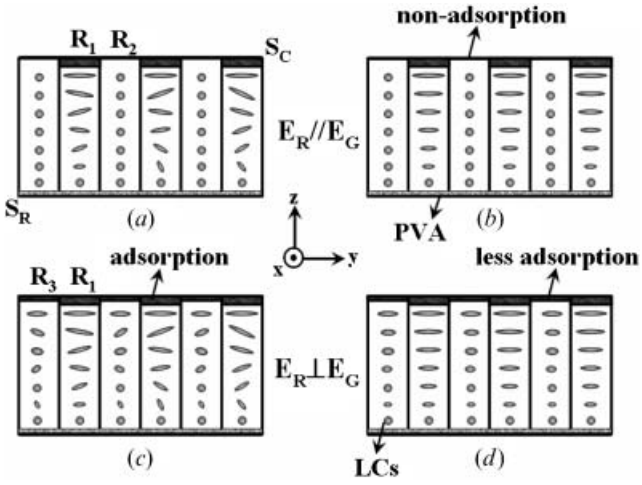

Figure 3. (*a*) and (*b*) [(*c*) and (*d*)] show side-view illustrations of anisotropic patterns in the BIHGs under the condition $E_R//E_G$ [$E_R \perp E_G$]. Also, (*a*, *c*) [(*b* are with[without] the bulk effect. R_1, R_2 and R_3 regions, represent E_G regions (which have strong adsorption of dye), E_R+E_G regions with $E_R//E_G$ (which have no significant dye adsorption) and E_R+E_G regions with $E_R \perp E_G$ (which have dye adsorption levels between the R_1 and R_2 regions).

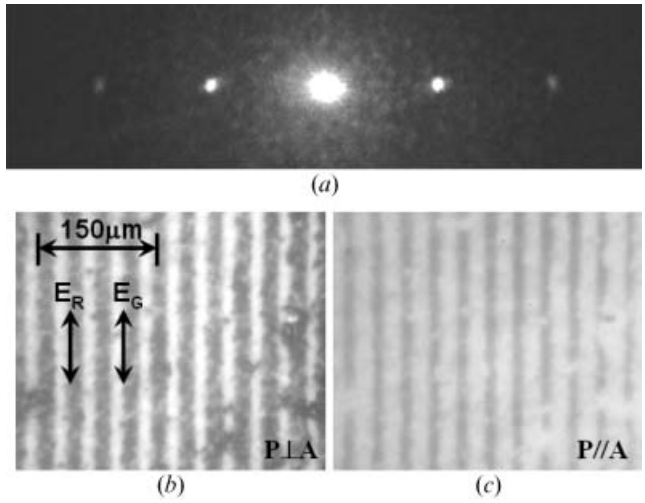

Figure 4. (*a*) Diffraction pattern of a persistent BIHG probed using an He-Ne laser. The images of the formed BIHG with a spacing of ~36 μm observed using polarizing optical microscopy under (*b*) crossed and (*c*) parallel polarizers. P and A are the transmissive axes of the polarizer and analyser, respectively. The polarizations of the green and red pump beams, E_G and E_R, are parallel.

molecules. As mentioned above, the green(red) light-dominant regions are the bright(dark) regions, since green light promotes the adsorption of the excited dyes by *trans–cis* isomerization, whereas red light resists adsorption through the *cis–trans* inverse isomerization. As a result, the LCs alignments in the former(latter) regions are twisted(homogeneous), and are responsible for the bright(dark) regions of the formed BIHGs in figures 4 (*b*).

Figure 5 displays the dynamic variations in the first order diffraction efficiency of a BIHG produced at various green pump-beam intensities, I_G. The experimental set-up is similar to that in figure 2 with $E_R//E_G$. Figure 5 shows that the first order diffraction efficiencies of both the bulk reorientation and the surface adsorption gratings increase with I_G from 6 to 10 mW cm^{-2}. This result is reasonable because a DDLC cell pumped at a higher green pump-beam intensity at a fixed red pump-beam intensity yields a higher first order diffraction efficiency of a transient grating, because *trans*-rich/*cis*-rich modulation in the bulk is greater; also, the first order diffraction efficiency of a surface adsorption grating is higher because more dye is periodically adsorbed on the command surface, S_C. However, when the green pump-beam intensity exceeds a critical value around 10 mW cm^{-2}, the capacity of the red intensity-modulated interference field to restrain dye molecules from *trans* to *cis* isomerization decreases, reducing the transient grating because the *trans*-rich/*cis*-rich modulation in the bulk is reduced. Also, the surface adsorption grating is smaller because more dye is adsorbed uniformly on the S_C. Notably in curve (*f*), the bulk reorientation effect disappears as the green pump-beam intensity exceeds 15 mW cm^{-2}. This is reasonable, since the periodic *trans*-rich/*cis*-rich modulation in the bulk is poor under such relatively high green-beam intensities. The red intensity-modulated interference field cannot prevent the dye molecules from undergoing *trans–cis* isomerization, and dye molecules are adsorbed on S_C in the green-rich regions directly to induce primarily a surface-adsorption grating. The inset in figure 5 plots the variation of the measured recording time of the BIHGs with the green pump-beam intensity. Data are obtained at intensities of 7, 8, 10, 12 and 15 mW cm^{-2}. The recording time is defined as the time required for the first order diffraction efficiency to reach 0.18% after the pump-beams are turned on. Clearly, the recording time decreases(increases) as the green pump-beam intensity increases under(over) the critical intensity. This result is understandable, since increasing the green pump-beam intensity below the critical value accelerates the adsorption of the dye. However, when the green pump-beam intensity exceeds the critical value, the red intensity-modulated interference field cannot prevent the dye molecules from undergoing *trans–cis* isomerization, so the interference field in the formation of the BIHGs is worsened.

Figure 6 shows the measured thermal effect on the formation of a BIHG at ambient temperatures of 20, 25,

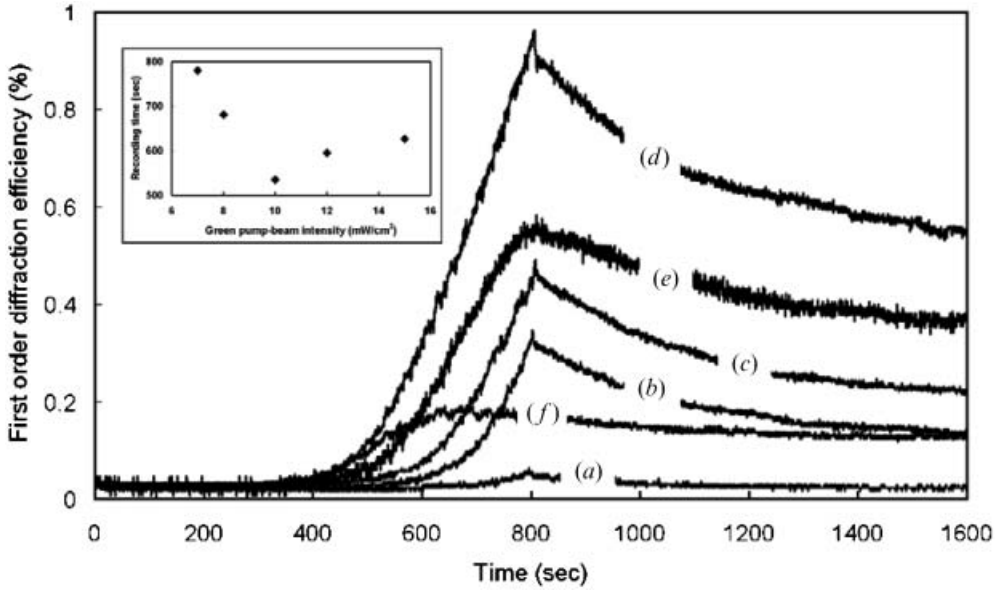

Figure 5. Variations of the dynamics of the first order diffraction during the formation of a BIHG with green pump-beam intensity at (*a*) 6, (*b*) 7, (*c*) 8, (*d*) 10, (*e*) 12 and (*f*) 15 mW cm^{-2}. The intensity of the red pump-beams is fixed at 180 mW cm^{-2}. All pump-beams, except for the probed beam, are turned on(off) at $t=0$ s (800 s). The inset presents the variation of the time to record BIHGs with the green pump-beam intensity.

30, 35 and 40°C. The intensities of the green and red pump-beams used were 8 and 180 mW cm^{-2}, respectively. In curves (*a*)–(*c*), all red and green beams were switched on and off at time $t=0$ and 600 s, respectively. The first order diffraction efficiencies in curves (*d*) and (*e*) are almost zero before time $t=1000$ s, so the DDLC film continued to be pumped without blocking all of the pump-beams. Figure 6 shows that the increase of ambient temperature reduces both the grating efficiency and the grating slope, indicating that more dye molecules are prevented from transforming from *trans*- to *cis*-isomers, and from adsorbing on the substrate.

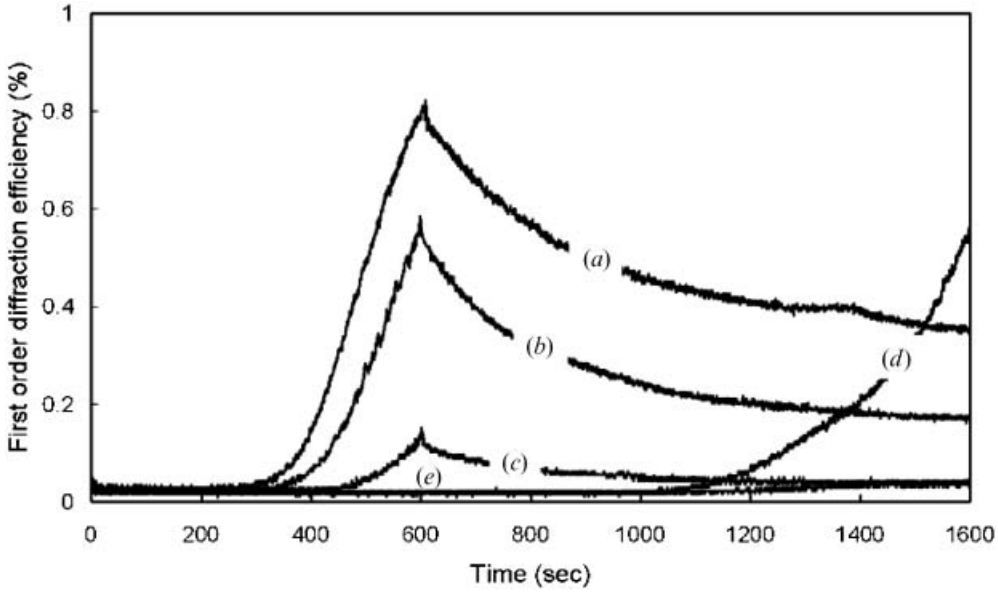

Figure 6. Variations in the dynamics of first order diffraction during the formation of a BIHG at ambient temperatures of (*a*) 20, (*b*) 25, (*c*) 30, (*d*) 35 and (*e*) 40°C. The intensities of the green and red pump beams are 8 and 180 mW cm^{-2}, respectively.

This is understandable, because heat can cause the dye molecules to isomerize in reverse from the *cis*-state to the *trans*-state. Additionally, thermal disturbance disorders the dye molecules and the LCs.

It should be noted in figure 6 that curve (*d*) shows a delayed initial response as compared with curves (*a*)–(*c*). This delay is caused by the fact that the ambient temperature of curve (*d*) (35°C) is close to the apparent clearing point ($T_{Ch\text{-}I}$) of the DDLC. In a separate experiment, it was verified that the clearing point of the DDLC cell with the illumination of the same green light intensity as in figure 6 is at ~38°C ($T_{Ch\text{-}I}$ of the nematic LC used, E7, is at ~61°C). The decrease of the clearing point for a nematic LC doped with dye is due to the photoinduced *cis*-isomers, which disorganize LC reorientation as reported in [15]. The same reason explains why no significant BIHG effect occurs at an ambient temperature of 40°C, curve (*e*).

4. Conclusions

This work investigates the optical and thermal effects on the dynamics of BIHGs based on DDLC films. A BIHG exhibits two effects; the bulk reorientation effect and the surface adsorption effect. The former yields a transient grating, whereas the latter results in a persistent grating. The results also indicate that the formation of a BIHG depends on the polarization direction of the green beams (E_G) relative to that of the red beam (E_R), the intensity of the green beam and the ambient temperature. The first order diffraction efficiency is much higher for $E_R // E_G$ than for $E_R \perp E_G$. The grating effect increases(decreases) as the green pump-beam intensity increases below(above) a critical intensity. Furthermore, a higher ambient temperature prevents more dye molecules from transforming from the *trans*-isomer to the *cis*-isomer, as well as from being adsorbed onto the substrate, reducing the BIHG effect.

Acknowledgement

The authors would like to thank the National Science Council (NSC) of the Republic of China (Taiwan) for financially supporting this research under contract no. NSC 94-2112-M-006-005.

References

[1] S. Slussarenko, O. Francescangeli, F. Simoni. *Appl. Phys. Lett.*, **71**, 3613 (1997).
[2] A.Y.-G. Fuh, C.-C. Liao, K.-C. Hsu, C.-L. Lu, C.-T. Tsai. *Opt. Lett.*, **26**, 1767 (2001).
[3] A.Y.-G. Fuh, C.-Y. Lu, T.-S. Mo, M.-S. Tsai. *Jpn. J. appl. Phys.*, **42**, 7344 (2003).
[4] E. Ouskova, Yu. Reznikov, S.V. Shiyanovskii, L. Su, J.L. West, O.V. Kuksenok, O. Francescangeli, F. Simoni. *Phys. Rev. E.*, **64**, 051709 (2001).
[5] W.M. Gibbons, P.J. Shannon, S.-T. Sun, B.J. Swetlin. *Nature*, **351**, 49 (1991).
[6] F. Simoni, O. Francescangeli. *J. Phys.: Condens. Matter*, **11**, R439 (1999).
[7] D. Voloschenko, A. Khizhnyak, Yu. Reznikov, V. Reshetnyak. *Jpn. J. appl. Phys.*, **34**, 566 (1995).
[8] K. Ichimura. *Chem. Rev.*, **100**, 1847 (1999).
[9] H. Fei, Z. Wei, P. Wu, L. Han, Y. Zhao, Y. Che. *Opt. Lett.*, **19**, 411 (1994).
[10] P. Wu, B. Zou, X. Wu, J. Xu, X. Gong, G. Zhang, G. Tang, W. Chen. *Appl. Phys. Lett.*, **70**, 1224 (1997).
[11] C. Sánchez, R. Alcalá, S. Hvilsted, P.S. Ramanujam. *Appl. Phys. Lett.*, **77**, 1440 (2000).
[12] C.-R. Lee, T.-S. Mo, K.-T. Cheng, T.-L. Fu, A.Y.-G. Fuh. *Appl. Phys. Lett.*, **83**, 4285 (2003).
[13] D. Statman, I. Jánossy. *J. chem. Phys.*, **118**, 3222 (2003).
[14] T.Ya. Marusii, Yu.A. Reznikov, S. Slussarenko. *Proc. SPIE Int.*, **2795**, 100 (1996).
[15] H.-K. Lee, K. Doi, H. Harada, O. Tsutsumi, A. Kanazawa, T. Shiono, T. Ikeda. *J. phys. Chem. B.*, **104**, 7023 (2000).
[16] G.H. Heilmeier, L.A. Zanoni. *Appl. Phys. Lett.*, **13**, 91 (1968).
[17] D.W. Berreman. *J. chem. Phys.*, **62**, 776 (1975).